

Intensity Scaling of Stimulated Raman Forward Scattering in Laser-Produced Plasmas

S. H. Batha,⁽¹⁾ D. S. Montgomery,⁽²⁾ K. S. Bradley,^{(2),(3)} R. P. Drake,^{(1),(3)} Kent Estabrook,⁽²⁾
and B. A. Remington⁽²⁾

⁽¹⁾*Plasma Physics Research Institute, University of California and Lawrence Livermore National Laboratory, Livermore, California 94550*

⁽²⁾*Lawrence Livermore National Laboratory, Livermore, California 94550*

⁽³⁾*Department of Applied Science, University of California, Davis, California 95616*

(Received 22 January 1991)

Measurement of the intensity scaling of stimulated Raman forward scattering (SRFS) at one observation angle is presented. A single, high-intensity 527-nm laser beam excited the instability in a preformed plasma whose properties are such that the predicted gain for SRFS spans the range anticipated for high-gain laser-fusion experiments. At low intensities, the gain of the instability was consistent with convective theory. At intensities greater than 1×10^{15} W/cm², the instability saturated at a level of less than 10^{11} W/sr nm cm².

PACS numbers: 52.40.Nk, 52.25.Rv, 52.35.Mw

Stimulated Raman forward scattering (SRFS) is a parametric instability whereby a strong pump beam interacts with a scattered-light wave and electron-plasma wave (EPW) in a feedback loop. Each "daughter" wave has a component of its group velocity that is parallel to the mean wave vector of the pump beam. The study of SRFS reported here is of particular interest to plasma physics as perhaps the first experimental study of a forward, three-wave parametric instability that is clearly not affected by coupling to backscatter.¹ Forward-scattering instabilities are believed to be inherently convective on theoretical grounds.² However, this conclusion has never, to our knowledge, been tested by experiment. Instead, experiments have most often studied backscattering processes, many of which can become absolutely unstable. This instability may become an important factor in designing high-gain laser-fusion targets where long electron-density scale lengths may lead to strong SRFS. Two possible detrimental consequences of SRFS are the production of suprathermal electrons and the scattering of light at large angles ($\approx 40^\circ$) which could degrade the illumination symmetry on a fusion pellet. The plasma regime of interest is high temperature (≈ 1 keV), low density ($\approx 0.02n_c$, where n_c is the laser critical density), and long scale length (greater than a few mm).

Early simulations and theory of SRFS emphasized its potential to produce suprathermal electrons,^{3,4} and experimentally observed suprathermal electrons were attributed to SRFS both in preliminary work⁵ and in the first report of a definitive observation of SRFS.⁶ The present work reports the first quantitative measurements of the scaling with pump intensity of the scattered light produced by SRFS, and compares these observations to predictions of the standard convective theory.

Attempts to understand the behavior of SRFS can be confused by coupling of this process to stimulated Ra-

man backscatter (SRBS) through propagation of the SRBS plasma wave to the density where it can seed SRFS. This coupling was believed to play a role in previous experimental⁶⁻⁹ and theoretical work.^{10,11} In the experiments reported here, this confusion was avoided in two ways. First, the plasma was warm enough that SRBS was quenched by Landau damping at the densities studied, and measurements during the SRFS detected no SRBS. Second, the plasma was large enough that even if SRBS had been present, the SRBS plasma wave would have been damped long before it could have reached the density at which it is resonant for SRFS.

The experiment measured the spectral power emitted at wavelengths corresponding to SRFS as a function of pump-laser intensity using a preformed plasma created by seven arms of the NOVA laser system¹² striking a 2 ± 0.1 - μ m-thick CH target. The target was a 2 ± 0.1 -mm-diam disk suspended on a 700- \AA -thick sheet of Formvar, which was at least 4 mm by 4 mm. Each side of the target was irradiated with about 7.5 kJ of 351-nm light in a 2 ± 0.2 -nsec-long, flat-top pulse with the irradiating, $f/4$, laser beams focused so that the overlap of each cluster of beams formed a roughly circular spot about 950 μ m in diameter.

The instability was driven by a high-intensity, $f/4$, 527-nm interaction beam at its best-focus diameter of 200 ± 25 μ m (defined to contain 80% of the laser power) with a depth of focus of ≈ 1 mm. The interaction pulse was delayed 200 psec after the end of the preform beams. The interaction beam, as well as the preform beams, struck the target at a 50° angle from the target normal. Intensity variation was produced by changing the energy in the interaction beam from a minimum of 100 J to a maximum of 2600 J. The interaction-beam pulse shape was determined on each experiment, and varied systematically with the interaction-beam energy. The intensities quoted in this work are the instantaneous

intensities at the time of SRFS emission. The pulse shapes at 527 nm were inferred from the measured pulse shapes and energies at the fundamental laser wavelength of $1.054 \mu\text{m}$ and the measured values of crystal conversion.¹³

The SRFS signal was measured with an absolutely calibrated^{14,15} 0.22-m optical spectrometer whose output was temporally resolved with a resolution of at best 2 nm and 50 psec. The relative accuracy of these measurements is estimated to be $\pm 50\%$, but the absolute accuracy is a factor of 3. The SRFS spectrometer was placed 27° from the forward direction of the interaction beam, 23° from the target normal, and 38° from the plane containing the electric-field and wave vectors of the interaction beam. In addition, the x-ray spectrum corresponding to bremsstrahlung from suprathermal electrons was monitored. No evidence for such electrons was found, as expected, because of their long mean free path in the low- Z plasma.

A typical SRFS spectrum is shown in Fig. 1. The wavelength of peak emission decreases with time, consistent with the expectation that SRFS will occur most strongly near the peak density in the plasma and that the peak density decreases with time. The SRFS emission occurs in bursts, turning on and off every 100 to 300 psec, consistent with the behavior observed by Turner *et al.*⁶ Only instrumental background signals are observed between bursts, implying that the emission has dropped at least a factor of 80. Temporal variations of the laser intensity cannot account for these bursts because in the linear regime of the instability, as can be deduced from Eq. (1), the laser intensity would have to vary by at least 45% over 100 to 300 psec. Such a large variation was not observed. In the saturated regime, even larger varia-

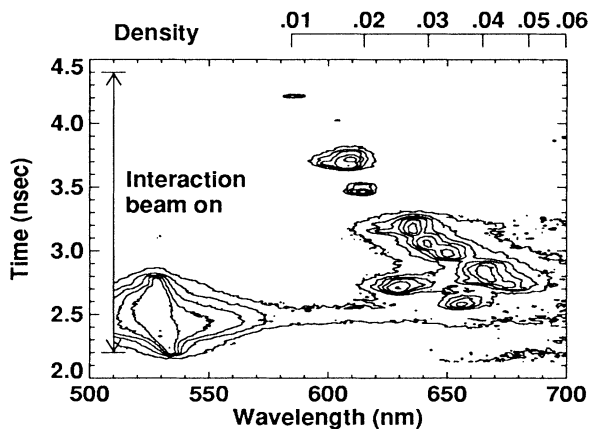


FIG. 1. Time-resolved spectrum in the SRFS signal in the saturated regime. The interaction beam intensity was $3 \times 10^{15} \text{ W/cm}^2$. The contours indicate factor of 2 variations in spectral power, with the highest contour at $2.6 \times 10^7 \text{ W/sr nm}$. A density scale, in units of the interaction-beam critical density, is shown at the top.

tions would be required. The onset is delayed 300 psec from the start of the interaction beam pulse. The observed spectral width is less than about 7 nm throughout and may be instrumental. Higher-resolution measurements will be needed to define the spectral shape. The signal at 527 nm is not due to SRFS. It began as soon as the interaction beam turned on (before the SRFS), lasted for 600 psec, and was so strong that it locally saturated the streak camera.

The experimentally measured spectral power (in W/sr nm) was converted to a gain factor by choosing the source of the SRFS to be the $200\text{-}\mu\text{m}$ -diam spot of the interaction beam and by choosing a background electron temperature based on simulations. An expression for the scattered-light flux,¹⁶ which accounts for plasma transmission of scattered light in the plasma, refraction, photon conservation, and thermal-noise level, was then solved for the exponential gain factor G . Errors in this calculation are estimated to be ± 0.9 in G . This analysis was performed for peak plasma densities of about $0.02n_c$. An arbitrary density could not be chosen because some of the experiments showed no amplification at some densities due to the intermittent behavior of the observed signals.

Figure 2 shows G as a function of intensity. At low intensities, a "convective-growth" region is identified where G increases with interaction-beam intensity. At intensities greater than about $1 \times 10^{15} \text{ W/cm}^2$, G increases less rapidly—the instability has saturated. Because the background plasma is very large (0.25 cm^2 was assumed) compared to the interaction region, G must be ≈ 5 before the signal will be observed above the thermal emission.

The theoretical gain factor for SRFS convective

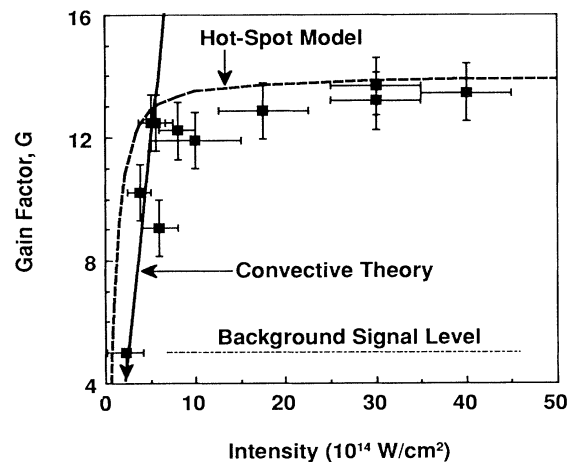


FIG. 2. Gain calculated from the measured fluence levels at $n = 0.02n_c$ at 3.6 nsec. The solid line is the convective gain calculated for the nominal intensity and the dashed line is the result of a hot-spot model where G saturates at 14.

growth at a density extremum has been calculated by Williams¹⁷ and is given by

$$G = A \left[\frac{\gamma_0}{(\kappa'')^{1/3} (V_{s,x} V_{EPW,x})^{1/2}} \right]^{3/2}, \quad (1)$$

where $V_{s,x}$ and $V_{EPW,x}$ are the components of the scattered-light wave and EPW group velocities along the density gradient (taken to be the target normal) and the second derivative of the wave-number mismatch along the density gradient is given by $\kappa'' = \omega_p / (2V_{EPW,x} L_g^2)$. The plasma frequency is ω_p . The homogeneous growth rate is defined to be

$$\gamma_0 = (k_{EPW} V_{osc}/4) (\omega_p^2 / \omega_s \omega_{EPW})^{1/2} |\cos \theta_p|,$$

where k_{EPW} is the EPW wave number, V_{osc} is the oscillatory velocity of an electron in the electron field of the laser, and ω_s (ω_{EPW}) is the scattered-light (EPW) frequency. The angle between the electric field vectors of the laser and the scattered light is θ_p ($=21^\circ$). The coefficient

$$A = \min \left\{ 7, 2\pi \left[\frac{\gamma_0}{v_{EPW}} \left(\frac{V_{EPW,x}}{V_{s,x}} \right)^{1/2} \right]^{1/2} \right\}, \quad (2)$$

where v_{EPW} is the combined Landau and collisional damping of the EPW, represents the effect of damping on the instability. The gain factor G is a strong function of observation angle (caused mainly by A), and has a maximum at some angle.¹⁸ The damping coefficient, in this experiment with a fixed observation angle, is only dominant for the lowest intensities and electron temperatures. The scaling of G for direct forward scatter is calculated to be $G \approx A I^{3/4} (n/n_c)^{7/8} T_e^{-1/4} \lambda_0^{1/2} L_g$, where λ_0 is the laser wavelength.

In evaluating this expression for an experiment, most quantities are determined either by the density inferred from the measured scattered-light spectrum, or by the geometry of the experiment. However, the values of the electron temperature T_e and Gaussian scale length, defined by $n(x) \equiv n_p \exp(-x^2/2L_g^2)$, where n_p is the peak density, are inaccessible with the available instrumentation. Instead, these were obtained from 2D hydrodynamic simulations using the computer code LASNEX.¹⁹

Confidence in the ability of LASNEX to accurately model these experiments was gained by comparing an unambiguously measured quantity, the peak electron density, with the code calculations in separate experiments that varied the shape and dimensions of the target.²⁰ It was found that the simulations, using flat-top laser pulses, reproduced the peak density very well, particularly between 2 and 4 nsec when the interaction beam was on. Initially, T_e is driven to ≈ 2.7 keV, and then decreases until it is below 1 keV at the end of the preform-beam pulse. Other simulations included the interaction beam beginning at 2.2 nsec with an energy of

either 2500 and 800 J. For the 2500 J (800 J) simulation, T_e is immediately driven to almost 2 (1.5) keV and then decays, beginning at about 2.5 nsec.

The electron-density scale length was calculated from the simulations by fitting a Gaussian profile to the calculated profile. During the interaction period, the scale length along the target normal, L_g , increased from about 0.15 cm to about 0.26 cm, and was largely independent of the interaction beam. The electron temperature varied from 0.4 to 1.1 keV, depending on interaction-beam intensity, while the scale length was assumed to be the same, 0.23 cm, in all cases.

The theoretical gain is shown as the solid curve in Fig. 2. The theory, when evaluated using the average laser intensity, and T_e and L_g from the simulations, accurately reproduces the measured gain for intensities below 1×10^{15} W/cm². We suspect that this good agreement may reflect offsetting errors, as follows. First, the effective scale length may be less than the assumed value because the plasma is not planar, which therefore reduces the gain proportionately at each intensity. Second, the effective laser intensity may be larger than the average value as the result of the distribution of intensities across the laser spot and along the beam waist, increasing the gain. As an example, the gain was recalculated assuming that the power distribution of the interaction beam was that of a spatially incoherent beam¹⁵ and that the gain factor saturated at 14. The result is shown as the dashed curve in Fig. 2 and bounds the experimental data quite well.

For intensities above 1×10^{15} , the instability was saturated. The present data allow only limited discrimination among possible saturation mechanisms, but some rudimentary estimates are indicative. For example, wave breaking is not a factor because $V_{osc}/V_{phase} \approx 0.1 < 1$, where V_{osc} is the oscillatory velocity of an electron in the incident laser electric field and V_{phase} is the EPW phase velocity.²¹ Additionally, trapping of electrons does not produce substantial damping because the simple criterion $V_{osc}/V_{phase} > 0.25(1 - 2V_{th}/V_{phase})^2$, where V_{th} is the electron thermal velocity, is not satisfied.²¹ Ion motion may be involved in the saturation dynamics, but whether this would be primarily via profile modification, Langmuir decay, or mode coupling is not clear. In addition, the two dimensionality of the electron density profile may limit the gain by limiting the size of the growth region for SRFS.

In conclusion, the gain of SRFS in a long-scale-length, low-density, CH plasma was measured. It was found that the onset and initial scaling with laser intensity of the spectral power of the SRFS corresponds to that predicted by convective theory, providing the first experimental evidence that such a theory may be correct for forward-scattering instabilities. At saturation, the amount of scattered light is relatively low. Future work should examine poorly understood features of the data,

including the onset of saturation, the signal level at saturation, the cause of the intermittent emission, and the spectral structure of the emission.

The authors would like to acknowledge useful discussions with J. Denavit, E. Hsieh, C. Laumann, W. L. Kruer, T. W. Johnston, R. E. Turner, T. Weiland, S. C. Wilks, and E. A. Williams. This work was performed under the auspices of the U.S. Department of Energy by the Lawrence Livermore National Laboratory under Contract No. W-7405-ENG-48.

¹The observations are far enough from direct forward scattering that the fourth, anti-Stokes plasma wave is not believed to be of primary importance.

²M. N. Rosenbluth, *Phys. Rev. Lett.* **29**, 565 (1972).

³Kent Estabrook, W. L. Kruer, and B. F. Lasinski, *Phys. Rev. Lett.* **45**, 1399 (1980).

⁴Kent Estabrook and W. L. Kruer, *Phys. Fluids* **26**, 1892 (1983).

⁵C. Joshi *et al.*, *Phys. Rev. Lett.* **47**, 1285 (1981).

⁶R. E. Turner *et al.*, *Phys. Rev. Lett.* **57**, 1725 (1986).

⁷H. Figueroa, C. Joshi, and C. E. Clayton, *Phys. Fluids* **30**,

586 (1987).

⁸D. M. Villeneuve and H. A. Baldis, *Phys. Fluids* **31**, 1790 (1988).

⁹C. Lobaune *et al.*, *Phys. Fluids B* **2**, 166 (1990).

¹⁰H. C. Barr, T. J. M. Boyd, and A. P. Mackwood, *Phys. Fluids B* **1**, 1151 (1989).

¹¹H. C. Barr, T. J. M. Boyd, and G. A. Coutts, *Phys. Rev. Lett.* **60**, 1950 (1988).

¹²E. M. Campbell *et al.*, *Rev. Sci. Instrum.* **57**, 2101 (1986).

¹³P. H. Chaffee and J. K. Lawson, in *Laser Program Annual Report 1987* (Lawrence Livermore National Laboratory, Livermore, CA, 1987).

¹⁴R. P. Drake *et al.*, *Phys. Rev. Lett.* **60**, 1018 (1988).

¹⁵R. P. Drake *et al.*, *Phys. Fluids* **31**, 3130 (1988).

¹⁶R. L. Berger, E. A. Williams, and A. Simon, *Phys. Fluids B* **1**, 414 (1989).

¹⁷E. A. Williams, in *Laser Program Annual Report 1985* (Lawrence Livermore National Laboratory, Livermore, CA, 1987).

¹⁸S. C. Wilks *et al.* (to be published).

¹⁹G. B. Zimmerman and W. L. Kruer, *Comments Plasma Phys. Controlled Fusion* **2**, 51 (1975).

²⁰S. H. Batha *et al.* (to be published); D. S. Montgomery *et al.* (to be published).

²¹T. P. Hughes, in *Laser Plasma Interactions*, edited by R. A. Cairns and J. J. Sanderson (SUSSP Publications, Edinburgh, 1980).